Journal of Applied Polymer Science

Development of Methods for Encapsulation of Viruses into Polymeric Nano- and Microparticles for Aquaculture Vaccines

Lilia S. Ulanova,[1]* Golnaz Isapour,[2]* Atoosa Maleki,[2] Shirin Fanaian,[2] Kaizheng Zhu,[2] Antje Hoenen,[1] Cheng Xu,[3] Øystein Evensen,[3] Gareth Griffiths,[1] Bo Nyström[2]

[1]Department of Molecular Biosciences, University of Oslo, N-0316 Oslo, Norway

[2]Department of Chemistry, University of Oslo, N-0315 Oslo, Norway

[3]Department of Basic Sciences and Aquatic Medicine, Norwegian School of Veterinary Science, Oslo, Norway

* Lilia S. Ulanova and Golnaz Isapour contributed equally to this work.

Correspondence to: B. Nyström (E-mail: b.o.g.nystrom@kjemi.uio.no)

ABSTRACT: To meet an urgent need for improved vaccines against viral diseases in aquaculture, encapsulating the viruses into biodegradable and biocompatible polymers was suggested to protect viral antigens from premature degradation and gradually expose them to the immune system. We used water-in-oil-in-water emulsion to first encapsulate model red fluorescent polystyrene (PS) particles and then infectious salmon anemia virus (ISAV) into poly-lactic-*co*-glycolic acid (PLGA) together with coumarin 6. A milder layer-by-layer method was applied to incorporate both PS and ISAV into chitosan (Cs)-fluorescein isothiocyanate and alginate (Alg) followed by ionic crosslinking. All particles were characterized by dynamic light scattering, zeta-sizer, fluorescence, transmission- and scanning electron microscopy. Successful encapsulation of PS beads and ISAV into PLGA, Cs, and Alg was accomplished. The prepared particles were of different size, surface charge density, and morphology. This yields opportunities for further developments of these structures as vaccine candidates to be delivered by injection or oral administration. © 2014 Wiley Periodicals, Inc. J. Appl. Polym. Sci. **2014**, *131*, 40714.

KEYWORDS: biocompatibility; biodegradable; biomaterials; biopolymers & renewable polymers; microscopy

Received 22 December 2013; accepted 4 March 2014

DOI: 10.1002/app.40714

INTRODUCTION

Numerous nano-engineering and chemical design studies have recently been carried out in controlled fabrication of nano-/micro-structured materials with tailored characteristics for vaccination and treatment purposes.[1–8] Encapsulation of molecules of interest into biodegradable polymers, e.g., poly-lactic-*co*-glycol acid (PLGA), chitosan (Cs), and alginate (Alg) offers many advantages over conventional methods of drug and vaccine delivery, such as controlled, sustained release, and specific targeting to the cells of interest.[9–11] The possibility of the particles to enter the application stage is defined by their size, encapsulation and loading efficiency, release profile, purity of preparation, and, importantly, the integrity/bioactivity of an active compound.[4,6,12,13] The particles gain additional value if they are specifically targeted so that they are delivered to the desired site by a certain mechanism.[4,13–15]

Biocompatible and biodegradable PLGA is perhaps one of the most promising hydrophobic polymers for fabrication of devices for drug delivery and vaccine candidates for human as well as for aquaculture use,[16,17] both in commercial and in research applications.[7,14,18] PLGA particles can be formulated in different sizes and modified to tailor them for desired applications and administration routes.[19] Different bacterial antigens (e.g., *Lactococcus garvieae*,[20] *Mycobacterium tuberculosis BCG*,[21] *Escherichia coli*,[22] *Vibrio cholerae*,[23] *Aeromonas hydrophyla*[17]), the whole viruses and viral antigens (infectious pancreatic necrosis virus,[22] influenza virus[24]), or DNA coding them have been successfully encapsulated into PLGA particles.[16]

Linear polysaccharide Cs also have found multiple applications in vaccines formulation due to its water-solubility, relative non-toxicity, biocompatibility, biodegradability, bioadhesive characteristics, and permeability enhancing properties.[25–30] Cs, a cationic polyelectrolyte derived from shellfish, is prepared from the deacetylation of chitin.[26,31] Cs-based particles possess different properties depending on the purity, molecular weight, degree of deacetylation, quality, and viscosity of the polymer. Such particles have been broadly studied for delivery of anti-cancer agents, therapeutic proteins, antigens and genes,[32] coding fish

bacterial (e.g. *Vibrio anguillarum*[33]), and viral antigens (Lymphocystivirus).[32,34,35]

Another promising polymer, a natural anionic polysaccharide obtained from brown algae, Alg, has often became a choice for making particulate formulations for aquaculture vaccination as this polymer possesses necessary properties such as biocompatibility, biodegradability, and muscoadhesivity.[26,36,37] Alg particles have been used in vaccination studies against various aquaculture pathogens, both bacterial (*Brucella melitensis*,[38] *Brucella abortus*,[39] *Flavobacterium*, *Aeromona salmonicida, L. garvieae, Streptococcus iniae, Vibrio Anguillarum*[17]) and viral (Lymphocystivirus,[34] infectious pancreatic necrosis virus[40]).

In this work, infectious salmon anemia virus (ISAV) was chosen as an example for application studies along with aforementioned polymers. This virus was first observed in diseased Atlantic salmon (*Salmon salar*) in Norway in 1984. ISAV infections cause enormous economic losses for global fish farming, especially in Canada, Chile, and Norway.[41,42] The current way of coping with viral infections in salmon aquaculture is through vaccines but there are currently few licensed vaccines against viral diseases.[43] Bacterial infections on the other hand are, with some exceptions, prevented through the use of inactivated, oil-based vaccines in salmon culture.[44] In this study, we have elaborated a basic technology that provides a rational foundation for the encapsulation of fish pathogenic viruses, such as ISAV into polymeric particles for the purpose of vaccination.

We investigate various methods for encapsulation of the chemically fixed ISAV particles into a number of biodegradable polymers, which are expected to protect their antigens from degradation until ISAV entities are taken up by antigen presenting cells; this eventually leads to tuning of the immune response.

In this study, we have focused on double emulsion solvent evaporation, layer-by-layer (LbL), and crosslinking (ionic gelation) methods.[5,7–11,13,14] The double emulsion solvent evaporation method has been widely used for the incorporation of hydrophilic compounds within the hydrophobic PLGA, though there are some concerns about the stability of the carriers after the contact with harsh solvents during the emulsification step.[6,13–15,31,36,41,42,45–48]

The LbL method offers an alternative strategy for making core particles that avoid these problems. This method is based on the electrostatic interactions between oppositely charged polyelectrolytes and it is fairly easy to perform on substrates of any shape.[1,2,8,13,23,28,46,49–51]

The above-described techniques allow formulation of relatively small particles, which can, for example, be used as vaccine candidates administered by injection. An alternative vaccine application that is addressed in this work is the preparation of particles for potential oral delivery. It is known that administration via this route is associated with poor bioavailability of the delivered vaccine candidate due to the degradation of the particles in the digestive tract. One of the most promising scenarios to avoid this phenomenon is to protect the biological molecules by employing polymeric carriers.[45,52] In addition, the particles that are to be naturally fed to fish have to be rather large and visible so the fish can recognize them as food. In other words, oral administration requires relatively large particle sizes. To accomplish this, ionic crosslinking gelation can be applied to formulate rather large beads and protect the active compound from fast premature degradation. This method allows the replacement of potentially toxic chemical crosslinker agents by physical ones, and to replace harsh organic solvents with aqueous ones.[25,26,31,45,53] This dramatically reduces the risk of the encapsulated biological molecules to be damaged.

To the best of our knowledge, this is the first study of polystyrene (PS) and fixed ISAV encapsulation in such systems. Our analysis here provides a strong foundation for further testing of nanoparticles and microparticles enclosing viruses for their efficacy in vaccination of aquaculture fish. We believe that these results demonstrate the power of these methods to encapsulate objects of different natures.

EXPERIMENTAL

Preparation of ISAV

A salmoniod cell line designated TO, originating from salmon head kidney leukocytes, was used at 20°C in L-15 medium (Invitrogen), supplemented with 5% fetal bovine serum (FBS), L-glutamine, and gentamicin.[54] The ISAV virus was propagated by inoculating confluent TO cells maintained with growth medium supplemented with 2% FBS. Culture supernatant was harvest at 14 days post infection when maximal cytopathic effect was developed. The virus was concentrated using Corning®Spin-X®UF Concentrators (100,000 MWCO) (Sigma Aldrich, St. Louis, MO) and the titer was determined by the 50% tissue culture infective dose (TCID50) method. The concentrated virus was inactivated with formalin (0.5%, vol/vol) for 72 h at room temperature. The mixture was then dialyzed against 100-fold volumes of phosphate buffered saline (PBS) using a Slide-A-Lyzer Dialysis Cassettes (10K MWCO, Thermo Scientific) over night at room temperature.

Synthesis of Fluorescein-5(6)-Isothiocyanate-Labeled Chitosan

The fluorescein-5(6)-isothiocyanate (FITC)-labeled low molecular weight Cs (Sigma-Aldrich (St. Louis, MO) with a degree of deacetylation of 75–85% (given by the manufacturer), $M_W = 9.0 \times 10^4$, and $M_w/M_n = 2.5$, both determined by asymmetric flow field-flow fractionation (AFFFF) methods as described in a previous study, was used.[55] The FITC was covalently attached to the polymer through a synthetic procedure reported elsewhere, with a minor modification.[56,57] Briefly, dehydrated methanol (100 mL) was added into the Cs solution (150 mL, 0.67% wt/vol in 1% vol/vol CH_3COOH), followed by 50 mL of FITC (90%, Sigma-Aldrich, St. Louis, MO) in methanol (2.0 mg/ml) under argon gas protection. Exposed to magnetic stirring and in the absence of light exposure (flask was covered with aluminum foil), the reaction was allowed to continue for another 24 h. The labeled polymer precipitated in 0.2*M* NaOH. The precipitated FITC-chitosan (FITC-Cs) polymer was centrifuged and washed repeatedly with a mixture of ethanol/water (70 : 30, vol : vol) till the bulk solution was free of FITC. The labeled Cs was re-dissolved in 100 mL of 0.1*M* CH_3COOH and dialyzed (dialysis cellulose membrane (MWCO, 8 kDa, Spectrum Laboratories) in the dark against water for 3 days, the water was replaced

with fresh water every 6 h. Finally, the labeled Cs was freeze-dried. Labeling efficiency 3.0 (% wt/wt FITC to FITC-Cs) was determined by measuring the absorbance intensity of the FITC-Cs solution against standard solutions of FITC using a UV–vis spectrometer.

Preparation of PLGA Particles by W/O/W Double Emulsion

Polystyrene latex beads (PS) (sulfate-modified PS, mean size is 100 nm, 2.5% solids ($\sim 4.7 \times 10^{13}$ particles/mL), contain red fluorescent dye with $\lambda_{ex}/\lambda_{em}$ ~575/610 nm, Sigma-Aldrich, St. Louis, MO) and ISAV (titer was 10^8 as determined by $TCID_{50}$ assay) were encapsulated in PLGA (50 : 50, 7000–17,000 kDa, Sigma-Aldrich, St. Louis, MO) particles separately according to a modified protocol of the double emulsion (W/O/W) solvent evaporation procedure described in previous studies.[13] Fluorescent PS latex beads served as a fluorescent model of ISAV since they both are negatively charged and exhibit similar size. Briefly, the prepared oil phase (O) consists of 2.6% of PLGA and 0.01% of coumarin 6 (Sigma-Aldrich, St. Louis, MO) in 15 mL dichloromethane (Sigma-Aldrich, St. Louis, MO) (DCM). The primary water phase (W) contains 3 mL of either an aqueous suspension comprising PS latex beads (0.02% solids, $\sim 7.8 \times 10^{10}$ particles/mL) or ISAV suspension. The primary W/O emulsion was created by mixing the oil and water phases using a magnetic stirrer (RH basic 2 IKAMAG®-IKA) for 2 min at 1200 rpm so as to force the interaction between PLGA and the particles to be encapsulated. In order to stabilize the primary emulsion, it was then added to 50 mL of 4% (wt/vol), polyvinyl alcohol (PVA), 87–90% hydrolyzed, average molecular weight 30,000–70,000 (Sigma-Aldrich, St. Louis, MO) under homogenization on ice (Homogenizer T 18 digital ULTRA-TURRAX®-IKA). For the first 45 s the homogenization speed was set to 11,000 rpm so as to avoid foaming and over-heating at the initial step. This was followed by homogenization at 24,000 rpm for the next 75 s to create smaller droplets. This approach resulted in particles with both decreased particle size and polydispersity index.[58,59]

After the secondary emulsification process described above, the suspension was stirred with a magnet bar at room temperature overnight to allow the evaporation of DCM. The next day particles were washed thrice with distilled water via centrifugation (Hettich Rotina 35, Hettich Zentrifugen, Tuttlingen, Germany) at 11,180 $\times$ *g* for 10 min at room temperature. About 2 mL of 0.5*M* sucrose was added each time during the washing process to reduce the tendency of aggregation and provide cryoprotection during further lyophilization.[5,60]

Preparation of Ionic Crosslinked Microparticles

Microparticles were prepared according to the protocol described elsewhere with some modifications.[25,53] Briefly, solutions of 3 wt % of low molecular weight alginic acid sodium salt (Sigma-Aldrich, St. Louis, MO) (Alg), with $M_w = 1.1 \times 10^5$ and $M_w/M_n = 3$, determined by AFFFF as described in a previous study was prepared.[55] The samples in distilled water or 3 wt % Cs in 1 vol/vol % acetic acid were prepared by stirring with a magnetic bar overnight at 500 rpm. Either an aqueous suspension of 200 μL of PLGA particles (formulated as described above) or PS beads suspension ($\sim 7.8 \times 10^{10}$ particles/mL) was gently mixed with either Alg or Cs solutions using a magnetic stirrer.

Aqueous solutions of the crosslinkers (0.05*M* $CaCl_2$ and 0.03*M* sodium tripolyphosphate (TPP) (Sigma-Aldrich, St. Louis, MO) were prepared shortly before the formulation of microparticles. Solutions of Cs or Alg were mixed with either PS beads or ISAV suspension, and then they were added drop-wise into the respective crosslinker's solution under magnetic stirring at room temperature. Microparticles were formed immediately and left for 1 h under stirring to harden. The particles were then washed three times with distilled water, spread on a mesh, and left to air-dry overnight.

Preparation of Nanoparticles by LbL and Ionic Crosslinking

Two types of core-shell ISAV nanoparticles were fabricated using the LbL assembly method and its combination with ionic crosslinking.[8,61] The principle of the method is based on electrostatic interactions between the oppositely charged core and the polymeric layers that assemble around it one by one forming an "onion-like" structure.

ISAV with negatively charged surface was used as a core and coated with positively charged Cs followed by coating with negatively charged Alg. The solutions of 0.1% Alg and Cs were prepared as described above with addition of 0.1*M* NaCl into the solvents to approach physiological conditions. Moreover, the salt ions prevent bridging effect and aggregation during the LbL procedure.[2,8] The solution of Cs contained 1/ 24 part of FITC-Cs to allow detection by fluorescent microscopy (FM). The pH of Cs solution was adjusted to 5 with several drops of 5*M* sodium hydroxide solution.[8]

The coating was performed at 4°C by drop-wise adding 200 μL of the ISAV suspension into the Cs solution under stirring at 600 rpm for 15 min. The suspension was then centrifuged at 25,000 $\times$ *g* for 10 min (Beckman Coulter Optima MAX Ultracentrifuge) and the supernatant was replaced by distilled water three times. After the third wash, 1 mL of the coated ISAV (ISAV-Cs) was added to the Alg solution under stirring and left for 15 min. The resulting sample (ISAV-Cs-Alg) was washed by centrifugation as described above. To make particles through a combination of LbL and ionic crosslinking methods, the ISAV suspension was first added to 0.05 wt % TPP solution and after vigorous stirring the suspension was immediately added to the 0.1 wt % Cs solution. The resulting suspension was kept inside an incubator for 15 min at $T = 4$°C to keep the particles at the most stable state and then washed three times by centrifugation (25,000 $\times$ *g*, 15 min, *T*: 4°C).[62]

Immunogold Labeling of ISAV and ISAV-Cs

The procedure was carried out on a clean surface of parafilm by transferring the grids between drops with different reagents. The primary antibodies were obtained from K. Falk (Department of Epidemiology, Norwegian veterinary Institute, Oslo), secondary antibodies were purchased from Genovac AG.

Characterization of the Particles

Transmission Electron Microscopy. The suspensions of particles were absorbed on hexagonal formvar grids for about 2 min, after that they were washed three times with MQ-water,

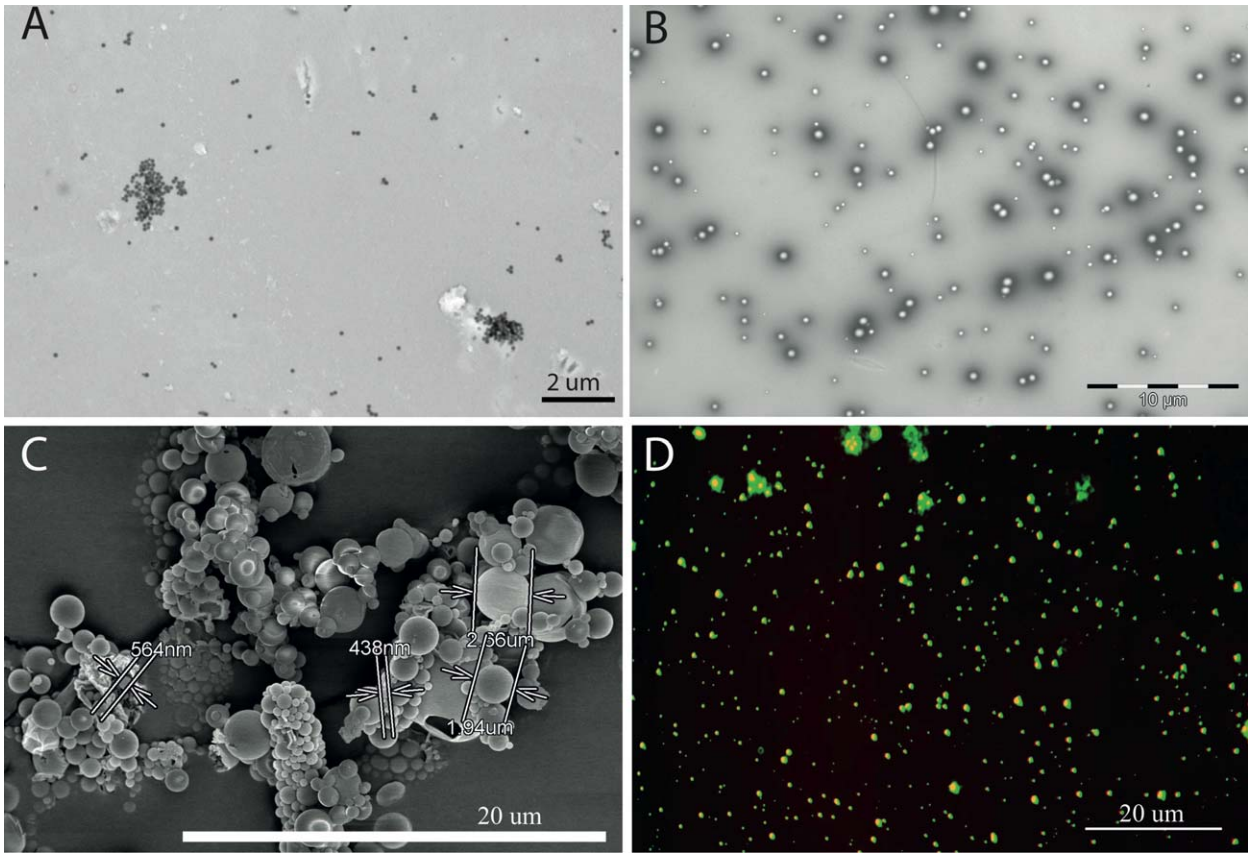

Figure 1. Microscopy images. (A) TEM of bare PS latex particles. (B) TEM of PLGA particles with encapsulated fluorescent PS particles. (C) SEM of encapsulated PLGA particles with PS-latex beads. (D) The merge of fluorescent micrographs of PLGA particles with encapsulated fluorescent PS particles taken at DS red (red) and GFP (green) channels. [Color figure can be viewed in the online issue, which is available at wileyonlinelibrary.com.]

stained with 3% uranyl acetate and then dried at room temperature. The imaging was performed with a Phillips transmission electron microscope CM100 (Philips, Eindhoven, The Netherlands). The images were recorded digitally with a Quemsa TEM CCD camera (Olympus Soft Imaging Solutions, Germany) and iTEM software (Olympus Soft Imaging Solutions, Germany).

Scanning Electron Microscopy. Freeze-dried particles were mounted on stubs using carbon tape and sputter coated with 4–6 nm platinum using a Cressington 308R coating system. Finally, the samples were examined and digital images were recorded using a Hitachi S-4800 field emission scanning electron microscope that operated at 5.0 kV.

Fluorescence Microscopy. Suspensions of particles were applied on a glass slide and then covered with a cover slip followed by imaging with an inverted fluorescent microscope Leica DM IRB (Leica Microsystems CMS GmbH, Wetzlar, Germany). The micrographs were taken using a digital camera, Leica DFC 365 FX (Leica Microsystems CMS GmbH, Wetzlar, Germany) and Leica Application Suite (LAS) V3.8. The processing of the micrographs was performed on a Fiji platform.[63]

Zeta Sizer. The zeta potential measurements were performed on a Malvern Zetasizer Nano ZS (Malvern Instruments Ltd., Worcestershire, UK). The ζ-potential was determined by the electrophoretic mobility of the samples at 25°C, using Laser Doppler Velocimetry. Each measurement was conducted in 12-mm glass cell PCS1115 cuvette with a cap using a dip-cell with palladium electrodes with 2 mm spacing. Each experiment was repeated three times and the average values are presented.

Dynamic Light Scattering. Dynamic light scattering (DLS) experiments were conducted by means of an ALV/CGS-8F multi-detector version compact goniometric system, with 8 fiber-optical detection units (ALV-GmbH, Langen, Germany). The beam from a Uniphase cylindrical 22 mW HeNe-laser, operating at a wavelength of 632.8 nm with vertically polarized light, was focused on the sample cell (10 mm NMR tubes, Wilmad Glass Co., of highest quality) through a temperature-controlled cylindrical quartz container (with 2 plane-parallel windows), which is filled with a refractive index matching

Table I. Surface Charge, Size Distribution, and Hydrodynamic Radius of the Studied Particles (β Size Distribution, R_h-Hydrodynamic Radius)

Sample	ζ-potential (mV)	β	R_h (nm)
ISAV	−16 ± 2mV	-	-
PLGA-blank	−2.0 ± 0.1	0.95	243
PLGA-PS	−2.07 ± 0.28	0.94	298
PLGA-ISAV	−3.03 ± 0.43	0.95	228

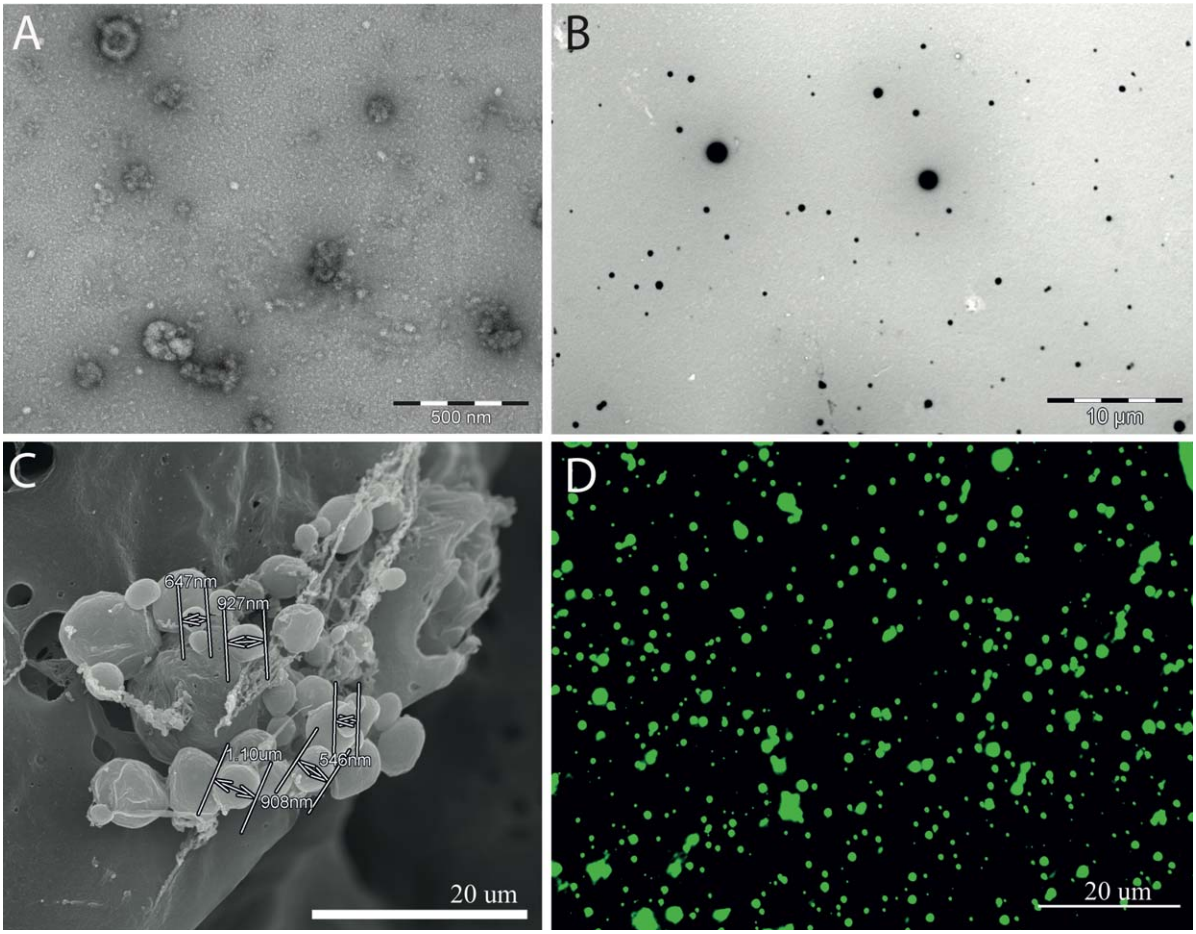

Figure 2. Microscopy images. (A) TEM of ISAV suspension. (B) TEM of PLGA particles with encapsulated ISAV. (C) SEM of PLGA particles with encapsulated ISAV. (D) FM of PLGA particles with encapsulated ISAV. [Color figure can be viewed in the online issue, which is available at wileyonlinelibrary.com.]

liquid (*cis*-decalin). The temperature in the container is controlled to within ±0.01°C with a heating/cooling circulator. The solutions were filtered in an atmosphere of filtered air through a 5 μm filter (Millipore) directly into pre-cleaned NMR tubes. The DLS experiments were performed at 25°C in the angular range of 22–141°.

The experimentally recorded normalized intensity autocorrelation function $g^2(q,t)$ is directly linked to the theoretically amenable first-order electric field autocorrelation $g^1(q,t)$ through the Siegert[64] relationship $g^2(q,t)=1+B|g^1(q,t)|^2$, where B (≤ 1) is an instrumental parameter and q is the wave vector $q=(4\pi n/\lambda)\sin(\theta/2)$, with λ, θ, and n being the wavelength of the incident light in a vacuum, scattering angle, and refractive index of the medium, respectively.

In suspensions of monodisperse particles, the correlation function can be described by eq. (1):

$$g^1(t)=\exp\left[-(t/\tau_e)^{\beta}\right] \quad (1)$$

where τ_e and β ($0<\beta\leq 1$) are the effective relaxation time and a measure of the width of the distribution of relaxation times, respectively. The mean relaxation time is given by

$$\tau=\frac{\tau_e}{\beta}\,\Gamma(1/\beta) \quad (2)$$

where $\Gamma(x)$ is the gamma function. Correlation functions are found to be diffusive (q^2-dependent) for all samples, i.e., $D=(1/\tau)/q^2$, where D is the mutual diffusion coefficient. The apparent hydrodynamic radii R_h of the particles can be calculated by using the Stokes–Einstein relationship[65]

$$R_h=\frac{k_B T}{6\pi\eta D} \quad (3)$$

where k_B is the Boltzmann constant, T is the absolute temperature and η is the viscosity of the solvent.

RESULTS AND DISCUSSION

PLGA Nanoparticles

The mean diameter of the PS beads given by the manufacturer is 100 nm; by transmission electron microscopy (TEM) we found them to range between 85 and 110 nm [Figure 1(A)]. The ζ-potential was measured to be −60 mV. Although, the surface properties of ISAV and PS particles may differ, the size of the particles is in the same range and they are both

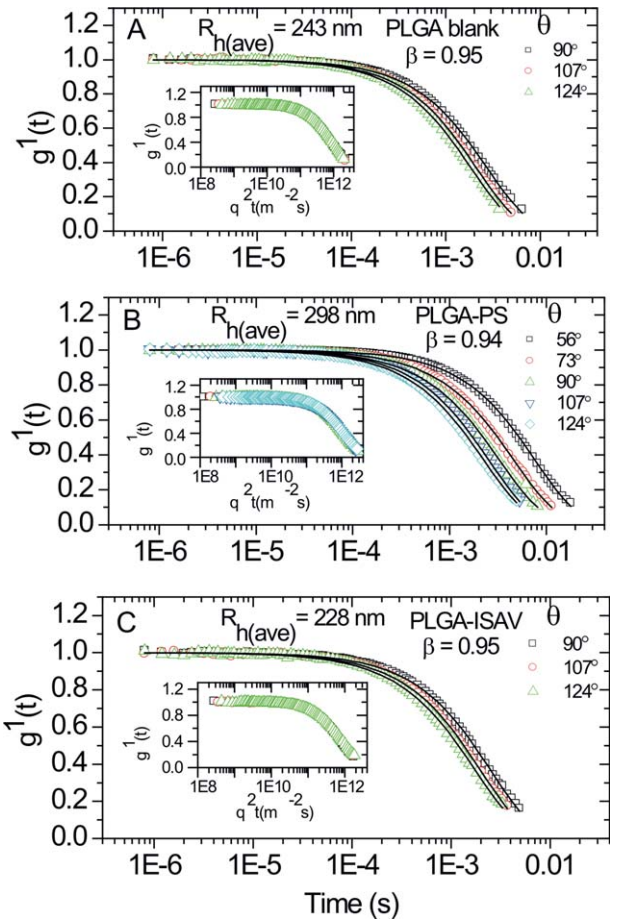

Figure 3. First-order electric field correlation function versus time for aqueous suspension of (A) PLGA-blank particles, (B) PLGA-PS particles, (C) PLGA-ISAV particles. Only the angles with less noise in correlation functions have been used for calculation of the sizes. The inset plots show q^2 dependency of correlation functions and the systems are shown to be diffusive. The particles were re-suspended in buffer with pH 7.4. [Color figure can be viewed in the online issue, which is available at wileyonlinelibrary.com.]

negatively charged (Table I). In view of this, PS beads were chosen as a suitable reference model for ISAV. These PS particle experiments were needed before proceeding to ISAV encapsulation, since the virus production was limited due to the complexity of the procedure.

Red fluorescent PS beads were successfully encapsulated into PLGA, with the addition of the fluorescent dye coumarin 6. The average size of the resulting particles was in the range 130–530 nm ($\beta = 0.94$), which exceeds the size of the naked PS beads [Figure 1(B) and Table I]. Some particles below or above the average size were formed due to the nature of emulsification process but they presented only a small fraction of the total particle population.

Scanning electron microscopy (SEM) revealed smooth surface of the PS-PLGA particles with no visible pores on it [Figure 1(C)]. The same morphology has been shown previously for PLGA particles with encapsulated proteins.[13] The successful encapsulation of PS beads in PLGA/coumarin 6 matrix was detected by FM [Figure 1(D)]. The micrographs were taken in DS red and GFP channels, their overlapping in Fiji software resulted in a yellow color where red fluorescent PS beads were detected inside the green fluorescent polymer matrix. No aggregation of the particles was observed.

All the PLGA particles we made with either encapsulated PS beads or ISAV had less negative surface charge than the PS beads and ISAV themselves, and the surface charge of all the PLGA particles were similar to the blank PLGA particles (Table I). This implies that most, if not the whole, surface of the encapsulated particles is composed of PLGA and PVA, indicative of successful encapsulation.

After establishing the use of the emulsion method to encapsulate an object with properties similar to ISAV into a PLGA matrix, we proceeded to the encapsulation of the fixed ISAV itself. The diameter of ISAV estimated by means of TEM was in the range 80–100 nm [Figure 2(A)]. The ζ-potential was -16 ± 2 mV (Table I), which together with surface morphology

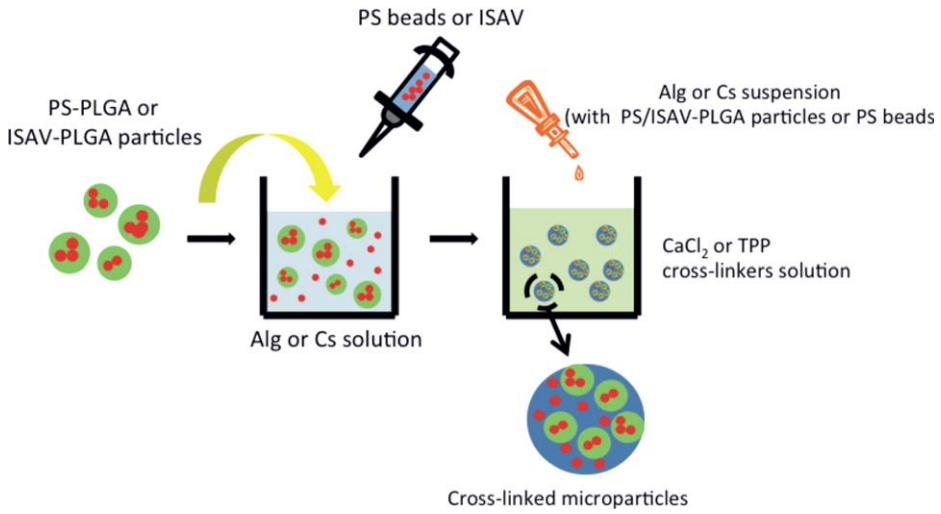

Figure 4. Schematic description of the crosslinked microparticles preparation. [Color figure can be viewed in the online issue, which is available at wileyonlinelibrary.com.]

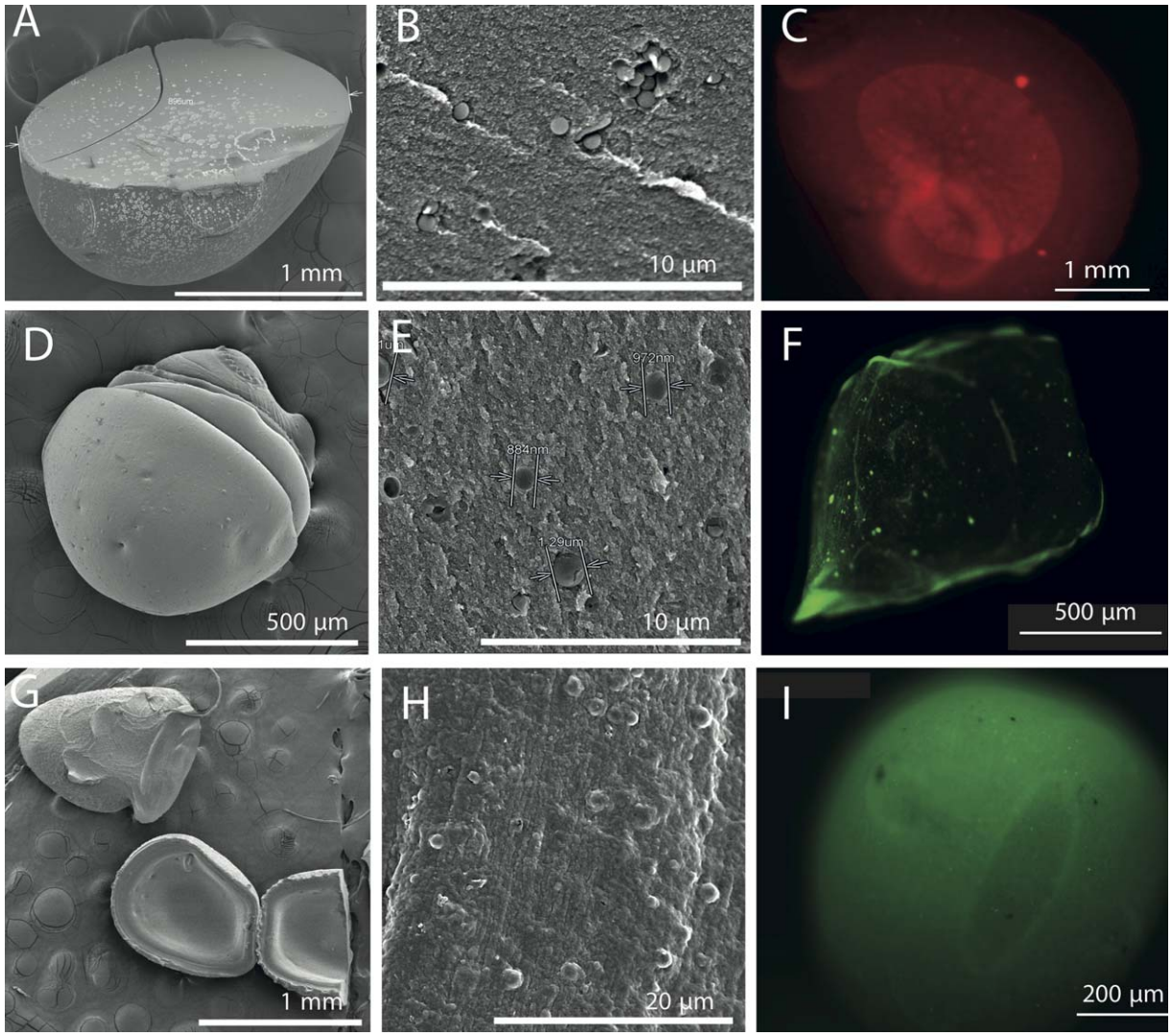

Figure 5. Microscopy images of crosslinked microparticles: (A) Alg.Cs.PS/SEM/ cross-section, (B) Alg.Cs.PS/SEM, cross-section inner surface, (C) Alg.Cs.PS/FM/whole particle, (D) Alg.Cs. PLGA-ISAV/SEM/whole particle, (E) Alg.Cs.PLGA-ISAV/SEM, cross-section inner surface, (F) Alg.Cs.PLGA-ISAV/FM/whole particle, (G) Cs.TPP.PLGA-ISAV/SEM/both whole and cross-section, (H) Cs.TPP.PLGA-ISAV/SEM, cross-section inner surface, (I) Cs.TPP.PLGA-ISAV/FM/ whole particle. [Color figure can be viewed in the online issue, which is available at wileyonlinelibrary.com.]

may be the reason for the frequently observed aggregation of ISAV [Figure 2(A)].[4] To reduce this aggregation tendency, gentle shaking of the virus suspension with a vortex was applied in the first step of particle production, before it was added to the polymer solution. The mean size of ISAV-PLGA particles prepared by the W/O/W double emulsion method was estimated to be ~450 nm [Figure 2(B), Table I] by TEM and DLS. However, individual larger particles up to 2–3 µm could be observed by SEM [Figure 2(C)] but they were not detected by TEM FM imaging demonstrated no significant aggregation of the ISAV-PLGA particle suspension [Figure 2(D)].

Table II. Characterization of the Nanoparticles Made by the LbL Method

Sample	Size (nm)	ζ-potential (mV)
ISAV	169 ± 14	−16 ± 2
ISAV-Cs	430.7 ± 8	+39 ± 1
ISAV-Cs-Alg	773 ± 155	−65 ±1

All the measurements were performed on the zeta-sizer.

Though a similar negative ζ-potential value has been reported for other types of PLGA particles, the surface charge of the particles formulated in this study was close to neutral due to partial annihilation of the charges.[66] The zeta potential measurements were performed in 0.1*M* NaCl solution in order to mimic physiological conditions. The presence of the salt ions in the PLGA particles suspension resulted in screening of the particles surface charge.

The determination of particle sizes (average hydrodynamic radius) and the width of the distribution of relaxation times (β value) were performed by the DLS technique. This is a powerful

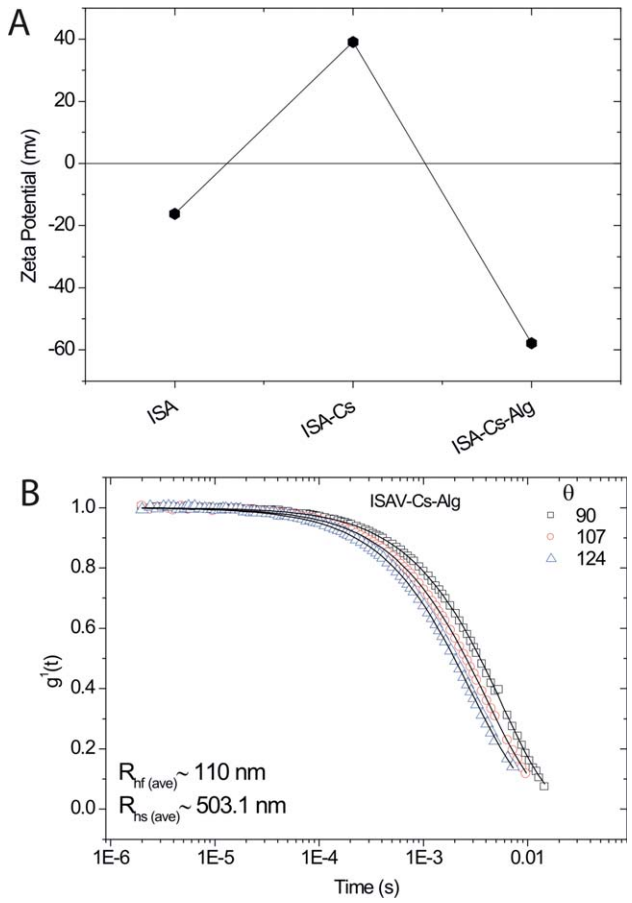

Figure 6. (A) Changes in ζ-potential during the assembly of Cs and Alg on ISAV, (B) time evolution of the first-order electric field correlation function for aqueous suspension of ISAV-Cs-Alg. [Color figure can be viewed in the online issue, which is available at wileyonlinelibrary.com.]

tool to probe relaxation processes and calculating the corresponding hydrodynamic radius of the particles.

The DLS measurements are summarized in Table I and depicted in Figure 3, where the normalized time correlation function data for the PLGA-blank, PLGA-PS, and PLGA-ISAV at the scattering angles indicated are displayed in the form of semi-log plots. The decays of the correlation functions are portrayed by a single stretched exponential [eq. (2)]; the inset plots (Figure 3) show that the systems exhibit a diffusive behavior. The distribution of relaxation times for the present systems displayed values of β $(0 < \beta \leq 1)$ in the range of $\beta = 0.94$–0.95, confirming that the size distribution of the suspension is fairly narrow. The size of the blank particles was close to that of the PS beads and ISAV encapsulated PLGA particles. The DLS data are in good agreement with the TEM measurements. In summary, the emulsion evaporation method allowed us to successfully make PS-composite particles with mean sizes of 450–600 nm, relatively low polydispersity index and slightly negatively charged. Zeta-potential, fluorescent, transmission and scanning electron microscopy measurements confirmed the encapsulation.

In summary, our results confirm that both PS beads and ISAV can be successfully encapsulated into PLGA nanoparticles using the emulsion solvent evaporation method. This finding is in agreement with previous studies.[3,5,6,13] Even though the used technique is not flawless, we have demonstrated that different size, morphology, and size distribution can be tuned by changing various parameters during the fabrication of the particles.[3,6,13,14,67] In this way the particles can be considered for different applications.[6,68]

Crosslinked Microparticles

In this work, we also discuss the preparation of microparticles that are intended to be included into fish food, and under specific temperature and pressure conditions they are cut into pellets or flakes so the fish can easily see and take the protected antigen.[33,69,70] In this section, we will discuss the preparation of such crosslinked microparticles.

In this context, PS beads and ISAV encapsulated into PLGA nanoparticles were incorporated into the larger microparticles.[45,52] This was accomplished by ionic crosslinking of Cs or Alg in solutions, using the frequently employed non-toxic agents of TPP and $CaCl_2$, respectively.[25,53] A schematic description of the crosslinking procedure is depicted in Figure 4. Both Cs and Alg are recognized as biocompatible, bioadhesive, and biodegradable polymers with mucoadhesive properties, which is a considerable advantage for oral delivery.[26–31,36]

The resulting microparticles were examined by fluorescence and scanning electron microscopy. The Alg microparticles with encapsulated PS beads exhibited smooth surfaces with no visible pores [Figure 5(A)]; the cross-section of the particle shows the presence of encapsulated PS beads [Figure 5(B)]. FM showed that the red fluorescent PS beads were inside the microparticles [Figure 5(C)]. Encapsulation of ISAV-PLGA/coumarin 6 particles yielded similar properties as for the Alg microparticles, with smooth surfaces [Figure 5(D)]. The presence of ISAV-PLGA particles can be observed in the cross-section of the Alg particle [Figure 5(E)] since they are visible by FM [Figure 5(F)] as dots. Cs microparticles containing ISAV-PLGA/coumarin 6 nanoparticles have a different shape than those made of Alg [Figure 5(G)]. The cross-section image revealed the presence of ISAV-PLGA nanoparticles inside the Cs microparticles [Figure 5(H)], and this is further accentuated by FM [Figure 5(I)]. All the formulated microparticles had size of ~1000 μm in diameter.

Successful encapsulation of both naked PS beads and ISAV-PLGA nanoparticles into microparticles opens the opportunity for these two approaches to be combined in future studies. Naked fixed ISAV particles can be encapsulated into Cs or Alg microparticles along with ISAV-PLGA particles. Thus the naked ISAV may be released earlier than ISAV from the PLGA matrix, providing gradual exposure of the viral antigens to the immune system.

Nanoparticles Prepared by LbL and Ionic Crosslinking

LbL assembly is an alternative approach for making core-shell nano- or microparticles. This method allows particles preparation without exposing the sample to shear forces and employing organic solvents, which may lead to loss of ISAV antigenicity.[6,66] The LbL method is based on electrostatic forces between

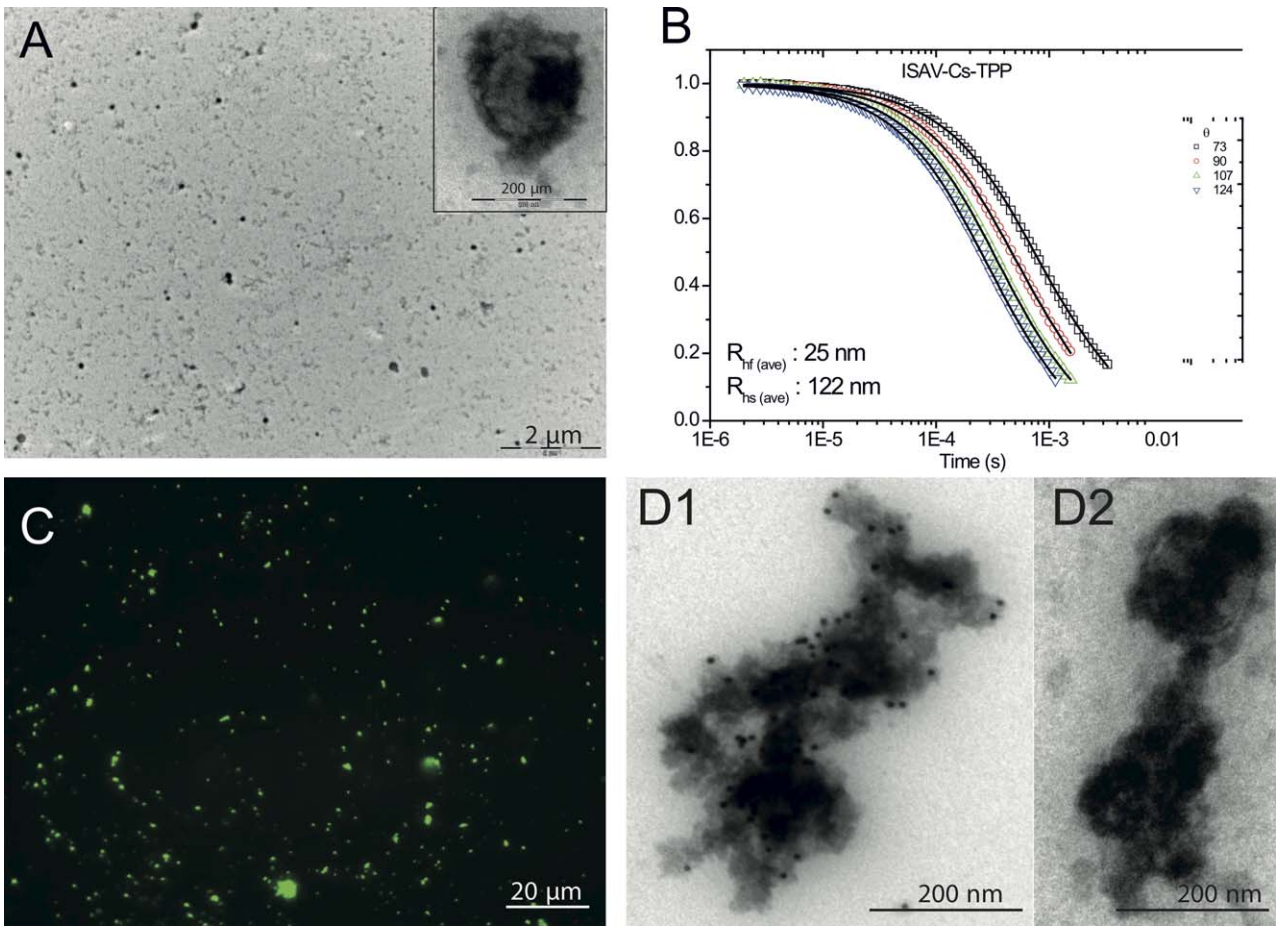

Figure 7. (A) Transmission electron micrograph of ISAV-Cs-TPP suspension and a single ISAV-Cs-TPP particle in the inlet. (B) Time evolution of the first-order electric field correlation function for aqueous suspension of ISAV-Cs-TPP. (C) FM of ISAV-Cs-TPP, green color is FITC-Cs exhibited in the system, (D1) Transmission electron micrograph of ISAV immunolabeled with 10 nm gold, (D2) transmission electron micrograph of ISAV-Cs-TPP shows the absence of immunolabeling. [Color figure can be viewed in the online issue, which is available at wileyonlinelibrary.com.]

oppositely charged layers. The LbL approach was utilized to encapsulate ISAV into Cs, where ISAV served as the negatively charged core that was coated with polycationic Cs, followed by a negatively charged Alg layer. The initial surface charge of ISAV was -16 ± 2 mV [Table II, Figure 6(A)] but after the deposition of the Cs layer the resulting zeta-potential changed to $+39 \pm 1$ mV, which in turn dropped to -65 ± 1mV after addition of the Alg layer (Table II).

The diameter of the resulting particles measured by the zetasizer at a scattering angle of 173° (Table II) increased by ~300 nm with each layer.

The correlation functions during DLS measurements of ISAV-Cs-Alg were found to be bimodal [Figure 6(B)]; a single exponential was followed at longer times by a stretched exponential.[71,72] This indicates that there are two populations of particles in the system—the fast mode represents small particles ($R_{hf} \approx 220$ nm) whereas the slow mode portrays the existence of larger particles ($R_{hs} \approx 1006$ nm). Both modes were diffusive (q^2-dependent).

The bimodal size distribution (high polydispersity) of ISAV-Cs-Alg particles in the suspension may be ascribed to the rather low charge density; therefore they may have a higher tendency to form aggregates as already mentioned in the discussion above. Another scenario that may come into play is the existence of extra Cs and Alg polymers in the system after the washing step, and this may induce aggregation of the two oppositely charged polyelectrolytes.

In addition to establish a polyelectrolyte deposition, the ζ-potential serves as an important index for the stability of the nanoparticle suspensions. Values of the ζ-potential above +30 mV or below −30 mV are believed to be strong indicators of electrostatic stabilization of the particles, via repulsive forces among the particles, which prevents aggregation.[4,73] Even though the ζ-potential of our ISAV was quite low (−16 mV), we could nevertheless successfully coat its surface with positively charged Cs, which resulted in surface charge that could stabilize the system and allow the deposition of another layer (Table II). Quinn et al. discussed the possibilities of multilayer formation of thin films through non-electrostatic interactions, including hydrogen bonding and hydrophobic interactions.[51,74,75] By employing these interactions, a host of different materials, with low or neutral surface charge, has been successfully incorporated into multilayer films.[51] Therefore, the assembly of Cs layer onto

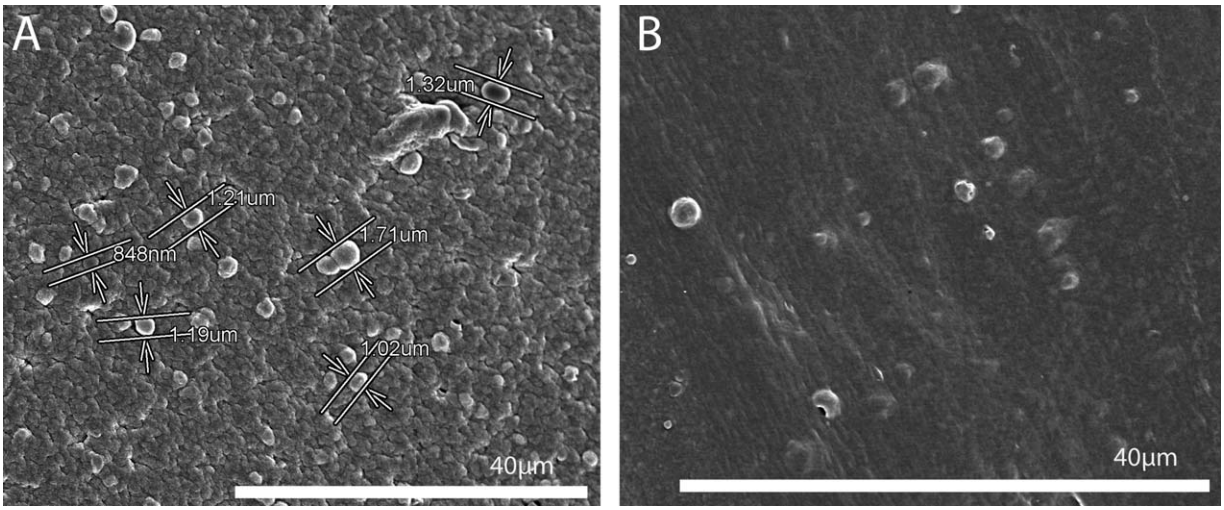

Figure 8. Scanning electron microscopy images of the surface of large crosslinked particles (A) Alg.Cs.PLGA/ISAV, (B) Cs.TPP.PLGA/ISAV.

ISAV could be mediated not only by electrostatic interactions, even though they are believed to contribute mostly, but due to the combined forces of several types of physical interactions.

Another series of ISAV-core particles was formulated by the combination of the LbL method and using the crosslinking agent TPP.[31,57] This process of controlled gelation of Cs resulted in the formation of spherical, homogenous, and compact nanoparticles. The size of these nanoparticles is smaller in comparison to the corresponding ones that are not crosslinked. The diameter is estimated to be ~200 nm by TEM [Figure 7(A)] and 242 nm by DLS [Figure 7(B)]. Both intra- and intermolecular crosslinking probably affect the reduction of the particle size. The detected particles of very small size ($R_{hf} = 25$ nm) may be due to the presence of Cs excess that became crosslinked. No aggregation was observed by FM [Figure 7(C)]. It is important to mention that FM cannot be used as a reliable and precise method for the particle size estimation as the objects often look few times bigger than they actually are. The sizes that one sees on fluorescent macrographs are highly affected by inherent characteristics of fluorophores, such as brightness and degree of quenching of the fluorescent signal.

Additional proof of ISAV encapsulation has been demonstrated by immunolabeling. The bare ISAV was possible to label with 10 nm gold [Figure 7(D1)], while the coated ISAV (ISAV-Cs-TPP) did not get labeled, most likely because of unavailability of the surface antigens covered with the polymer [Figure 7(D2)].

These results suggest that LbL is a suitable method for encapsulation of biological objects (e.g., viruses) into Cs and Alg shell. Furthermore, this method is very mild and excludes the problem of the encapsulated virus antigenicity loss caused by harsh conditions. LbL is a very flexible method and allows creation of particles of many different compositions.

CONCLUSIONS

This study demonstrated the possibility of encapsulation of PS beads and ISAV into several biocompatible and biodegradable polymers. The W/O/W emulsion solvent evaporation method was used to prepare PLGA nanoparticles of sizes less than one micron with smooth and negatively charged surfaces. The LbL method[8] used for the preparation of ISAV coated with Cs and Alg was milder and did not require the use of harsh solvents, which may damage the encapsulated ISAV. The size and surface charge of the particles manufactured by the LbL method could be controlled by the choice of the polymers and number of coating layers. Additional crosslinking of the particles may enhance their stability. Both types of particles formulated by W/O/W emulsion solvent evaporation and LbL methods had relatively small sizes and thus could potentially be used as vaccine candidates delivered by injections.

The beads formulated by ionic crosslinking of Cs and Alg are shown to contain the encapsulated PLGA particles (Figure 8) and to be approximately 1 mm in diameter.[25,53] Such design of the particles helps to avoid rapid ISAV release by providing the antigens with a double protection. All this makes the Alg and Cs beads potential candidates for oral vaccines.

In summary, three formulation methods were shown to be suitable for making aquaculture vaccine candidates with various properties and aimed for different routes of administration. The encapsulation of PS and ISAV by all methods was successful, which opens a variety of options for tailor-made particle formulation. Depending on the choice of polymers, the resulting particles may in the future be adapted for more specific requirements of the aquaculture industry. Thus the performed study lays a solid foundation for further vaccines development.

ACKNOWLEDGMENTS

This research project was supported by Inven2 and the FORNY program ("Nanobead vaccine delivery platform for aquaculture", project no. 208297/O30) through the Norwegian Research Council. Authors acknowledge the Electron Microscopy Facility at University of Oslo for providing the opportunity of EM imaging.

AUTHORS CONTRIBUTION STATEMENT

Lilia S. Ulanova planned the experiments, provided training and supervision during preparation of the particles by W/O/W emulsion and LbL methods, performed LbL technique for encapsulation of ISAV and PS particles and characterized the resulting formulations, did all the imaging except for SEM, wrote the manuscript, and prepared the figure files. Golnaz Isapour prepared particles by W/O/W and ionic crosslinking methods, performed their characterization by zeta-sizer and DLS, contributed in writing and revising the manuscript. Atoosa Maleki planned the experiments, supervised most of the experiments and performed several of them, contributed to the manuscript and figures preparation. Shirin Fanaian conducted proof-of-principle experiments and modified LbL method. Kaizheng Zhu synthesized FITC-labeled chitosan. Antje Hoenen performed SEM imaging. Cheng Xu prepared ISAV suspensions and worked on increasing the yield of virus. Øystein Evensen supervised the virus preparation, acted as an advisor during experiments planning and the manuscript preparation. Gareth Griffiths participated in the planning of the experiments, supervised the general project development, contributed in writing and revising the manuscript. Bo Nyström significantly contributed to the manuscript writing and revision, provided the main supervision throughout the project, took care of both organizational and scientific parts of the project.

REFERENCES

1. Wang, A.; Tao, C.; Cui, Y.; Duan, L.; Yang, Y.; Li, J. *J. Colloid Interface Sci.* **2009**, *332*, 271.
2. Sukhorukov, G. B.; Donath, E.; Moya, S.; Susha, A. S.; Voigt, A.; Hartmann, J.; Möhwald, H. *J. Microencapsulation* **2000**, *17*, 177.
3. Wang, Y.; Jianzhi, Z.; Yuan, T.; Yanling, W.; Gong, H.; Xiaohui, L.; Jianxiang, Z. *J. Colloid Interface Sci.* **2013**, *394*, 573.
4. Haidar, Z. S.; Hamdy, R. C.; Tabrizian, M. *Biomaterials* **2008**, *29*, 1207.
5. Ye, M.; Kim, S.; Park, K. *J. Control. Release* **2010**, *146*, 241.
6. Nayak, B.; Panda, A. K.; Ray, P.; Ray, A. R. *J. Microencapsulation* **2009**, *146*, 241.
7. Makadia, H. K.; Siegel, S. J. *Polymers* **2011**, *3*, 1377.
8. Zhou, J.; Romero, G.; Rojas, E.; Ma, L.; Moya, S.; Gao, C. *J. Colloid Interface Sci.* **2010**, *345*, 241.
9. Couvreur, P.; Vauthier, C. *Pharm. Res.* **2006**, *23*, 1417.
10. Danhier, F.; Ansorena, E.; Silva, J. M.; Coco, R.; Le Breton, A.; Préat, V. *J. Control. Release* **2012**, *161*, 505.
11. Davis, M. E.; Chen, Z. G.; Shin, D. M. *Nat. Rev. Drug Discov.* **2008**, *7*, 771.
12. Han, L.; Zhao, J.; Zhang, X.; Cao, W.; Hu, X.; Zou, G.; Duan, X.; Liang, X. -J. *ACS Nano* **2012**, *6*, 7340.
13. Coleman, J.; Lowman, A. *J. Biomater. Sci*, **2012**, *23*, 1129.
14. Jiang, W.; Gupta, R. K.; Deshpande, M. C.; Schwendeman, S. P. *Adv. Drug Deliv. Rev.* **2005**, *47*, 391.
15. Solheim, E. *Int. Orthop.* **1998**, *22*, 410.
16. Cleland, J. L. *Tibtech January*, **1999**, *17*, 25.
17. Rivas-Aravena, A.; Sandino, A. M.; Spencer, E. *Biol. Res.* **2013**, *46*, 407.
18. Lü, J.-M.; Wang, X.; Marin-Muller, C.; Wang, H.; Lin, P. H.; Yao, Q.; Chen, C. *Expert Rev. Mol. Diagn.* **2009**, *9*, 325.
19. Tamber, H.; Johansen, P.; Merkle, H. P.; Gandera, B. *Adv. Drug. Deliv. Rev.* **2005**, *57*, 357.
20. Altun, S.; Kubilay, A.; Ekici, S.; Didinen, B. I.; Diler, O. *Kafkas Univ. Vet. Fak. Derg. (Suppl B)*. **2011**, *16*, 211.
21. Rice-Ficht, A. C.; Arenas-Gamboa, A. M.; Kahl-McDonagh, M. M.; Ficht. T. A. *Curr. Opin. Microbiol.* **2010**, *13*, 106.
22. Munang'andua, H. M.; Fredriksen, B. N.; Mutoloki, S.; Brudeseth, B.; Kuo, T.-Y.; Marjara, I. S.; Dalmo, R. A.; Evensen, Ø. *Vaccine* **2012**, *30*, 4007.
23. Yeh, M.-K.; Chiang, C.-H. *J. Microencapsulation* **2004**, *21*, 91.
24. Okamotoa, S.; Yoshii, H.; Akagid, T.; Akashid, M.; Ishikawa, T.; Okuno, Y.; Takahashi, M.; Yamanishi, K.; Mori, Y. *Vaccine* **2007**, *25*, 8270.
25. Wittaya-Areekul, S.; Kruenate, J.; Prahsarn, C. *Int. J. Pharm.* **2006**, *312*, 113.
26. Rinaudo, M. *Polym. Int.* **2008**, *57*, 397.
27. Fan, W.; Yan, W.; Xu, Z.; Ni, H. *Colloids Surf. B: Biointerfaces* **2012**, *90*, 21.
28. Ratajska, M.; Strobin, G.;Wisniewska-Wrona, M.; Ciechanska, D.; Struszczyk, H.; Boryniec, S.; Binias, D.; Binias, W. *Fibres Text. Eastern Eur.* **2003**, *11*, 42.
29. Felt, O.; Buri, P.; Gurny, R. *Drug Dev. Ind. Pharm.* **1998**, *24*, 979.
30. Saber, A.; Strand, S. P.; Ulfendahl, M. *Eur. J. Pharm. Sci.* **2010**, *39*, 110.
31. Dash, M.; Chiellini, F.; Ottenbrite, R. M.; Chiellini, E. *Prog. Polym. Sci.* **2011**, *36*, 981.
32. Janes, K. A.;Calvo, P.; Alonso, M. J. *Adv. Drug. Deliv. Rev.* **2001**, *47*, 83.
33. Rajesh Kumar, S.; Ishaq Ahmed, V. P.; Parameswaran, V.; Sudhakaran, R.; Sarath Babu, V.; Sahul Hameed, A.S. *Fish Shellfish Immunol.* **2008**, *25*, 47.
34. Zheng, F.-R.; Sun, X.-Q.; Liu, H.-Z.; Zhang, J.-X. *Aquaculture*, **2006**, *261*, 1128.
35. Ramos, E. A.; Relucio, J. L. V.; Torres-Villanueva, C. A. T. *Mar. Biotechnol. (NY)* **2005**, *7*, 89.
36. Lee, K. Y.; Mooney, D. J. *Prog. Polym. Sci.* **2012**, *37*, 106.
37. Sharma, S.; Mukkur, T. K. S.; Benson, H. A. E.; Chen, Y. *J. Pharm. Sci.* **2009**, *98*, 812.
38. Arenas-Gamboa, A. M.; Ficht, T. A.; Kahl-McDonagh, M. M.; Rice-Ficht, A. C. *Infect. Immun* **2008**, *76*, 2448.
39. Arenas-Gamboa, A. M.; Ficht, T. A.; Kahl-McDonagh, M. M.; Gomez, G.; Rice-Ficht, A. C. *Infect Immun* **2009**, *77*, 877.
40. de las Heras, A. I.; Saint-Jean, S. R.; Pérez-Prieto, S. I. *Fish Shellfish Immunol.* **2010**, *28*, 562.

41. Falk, K.; Aspehaug, V.; Vlasak, R.; Endresen, C. *J. Virol.* **2004**, *78*, 3063.
42. Thorud, K. E.; Djupvik, H. O. *Bull. Eur. Assoc. Fish Pathol.* **1988**, *8*, 109.
43. Biering, E.; Villoing, S.; Sommerset, I.; Christie, K. E. In Fish Vaccinology, Developments in Biologicals; Midtlyng, P. J. Ed.; Karger: Basel, Switzerland, **2005**; Vol. *121*, p 97.
44. Håstein, T.; Gudding, R.; Evensen, Ø. In Fish Vaccinology, Developments in Biologicals; Midtlyng, P. J. Ed.; Karger: Basel, Switzerland, **2005**; Vol. *121*, p 55.
45. Rieux, A. D.; Fievez, V.; Garinot, M.; Schneider, Y.-J.; Préat, V. *J. Control. Release Rev.* **2011**, *116*, 1.
46. Bergbreiter, D. E.; Liao, K.-S. *Soft Matter* **2009**, *5*, 106.
47. Xie, S.; Wang, S.; Zhu, L.; Wang, F.; Zhou, W. *Colloids Surf. B: Biointerfaces* **2009**, *74*, 358.
48. Morlock, M. K.;Winter, H. G.;Kissel, T. *Eur. J. Pharm. Biopharm.* **1997**, *43*, 29.
49. Shenoy, D. B.; Antipov, A. A.; Sukhorukov, G. B. *Biomacromolecules* **2003**, *4*, 265.
50. Cuomo, F.; Lopez, F.; Miguel, M. G.; Lindman, B. *Langmuir* **2010**, *26*, 10555.
51. Quinn, J. F.; Johnston, A. P. R.; Such, G. K.; Zelikin, A. N.; Caruso, F. *Chem. Soc. Rev.* **2007**, *36*, 707.
52. Joung, Y. K.; Choi, J. H.; Park, K. M.; Park, K. D. *Biomed. Matter* **2007**, *2*, 269.
53. Mi, F.-L.; Sung, H.-W.; Shyu, S.-S.; Su, C.-C.; Peng, C.-K. *Polymer* **2003**, *44*, 6521.
54. Wergeland, H. I.; Jakobsen, R. A. *Dis. Aquat. Org.* **2001**, *44*, 183.
55. Jonassen, H.; Kjøniksen, A.-L.; Hiorth, M. *Colloid Polym. Sci.* **2012**, *290*, 919.
56. Tallury, P.; Kar, S.; Bamrungsap, S.; Huang, Y.-F.; Tan, W.; Santra, S. *Chem. Commun.* **2009**, 2347.
57. Huang, M.; Khor, E.; Lim, L.-Y. *Pharm. Res.* **2004**, *21*, 344.
58. Sameni, J.; Bukhari, N. I.; Azlan, N. A.; Julianto, T.; Majeed, A. B. A. In 2009 IEEE Symposium on Industrial Electronics and Applications (ISIEA 2009), Kuala Lumpur, Malaysia, October 4–6, **2009**.
59. Freitas, S.; Merkle, H. P.;Gander, B. *J. Control. Release* **2005**, *102*, 313.
60. Abdelwahed, W.; Degobert, G.; Stainmesse, S.; Fessi, H. *Adv. Drug. Deliv. Rev.* **2006**, *58*, 1688.
61. Kim, B.-G.; Kang, I.-J. *Ultramicroscopy* **2008**, *108*, 1168.
62. Liu, H.; Gao, C. *Polym. Adv. Technol.* **2009**, *20*, 613.
63. Schindelin, J.; Carreras, I. A.; Frise, E.; Kaynig, V.; Longain, M.; Pietzch, T.; Preibisch, S.; Rueden, C.; Saalfeld, S.; Schmid, B.; Tinevez, J.-Y.; White, D. J.; Hartenstein, V.; Eliceiri, K.; Tomancak, P.; Cardona, A. *Nat. Methods* **2012**, *9*, 676.
64. Siegert, A. J. F. *MIT Rad. Lab. Rep. No. 465*, 1943.
65. Chu, B. Laser Light Scattering; Academic Press: USA, **1974**.
66. Gaumet, M.; Gury, R.; Delie, F. *Int. J. Pharm.* **2010**, *390*, 45.
67. Raghuvanshi, R. S.; Goyal, S.; Singh, O. M.; Panda, A. K. *Pharm. Dev. Technol.* **1998**, *3*, 269.
68. Romanski, F. S.; Winkler, J. S.; Riccobene, R. C.; Tomassone, M. S. *Langmuir* **2012**, *28*, 3756.
69. Romalde, J. L.; Luzardo-Alvárez, A.; Ravelo, C.; Toranzo, A. E.; Blanco-Méndez, J. *Aquaculture* **2004**, *236*, 119.
70. Tian, J.; Yu, J.; Sun, X. *Vet. Immunol. Immunopathol.* **2008**, *126*, 220.
71. Maleki, A.; Lafitte, G.; Kjøniksen, A.-L.; Thuresson, K.; Nyström, B. *Carbohydr. Res.* **2008**, *343*, 328.
72. Maleki, A.; Zhu, K.; Pamies, R.; Schmidt, R.; Kjøniksen, A.-L.; Karlsson, G.; Cifre, J. G. H.; de la Torre, J. G.; Nyström, B. *Soft Matter* **2011**, *7*, 8111.
73. Shiqu, Y. E.; Chaoyang, W.; Xinxing, L.; Zhen, T. *J. Biomater. Sci. Polym. Ed.* **2005**, *16*, 909.
74. Stockton, W. B.; Rubner, M. F. *Macromolecules* **1997**, *126*, 220.
75. Serizawa, T.; Hashaguchi, S.; Akashi, M. *Langmuir* **1999**, *15*, 5363.